Vortex glass melting in Mg-deficient MgB_2

A. A. M. Oliveira,[1,*] N. Hur,[2] S-W. Cheong,[2] and W. A. Ortiz[1]
[1]*Departamento de Física, Universidade Federal de São Carlos, 13565-905 São Carlos, SP, Brazil*
[2]*Rutgers Center for Emergent Materials and Department of Physics and Astronomy, Rutgers University, Piscataway, New Jersey 08854, USA*
(Received 29 December 2009; revised manuscript received 6 July 2010; published 8 September 2010)

In this paper we verify that clustering of Mg-deficient regions in superconducting $Mg_{1-x}B_2$ samples, introduces random disorder into the system, sufficient to stabilize a vortex glass phase for small enough values of x. Employing harmonic susceptibility, among other experimental techniques, we have conducted a systematic investigation of the glass-liquid frontier in the magnetic field versus temperature phase diagram of vortex matter for three samples, corresponding to $x=0.025$, 0.075, and 0.100. Interestingly, the studied melting line presents a kink in the low-field/high-temperature region of the diagram, indicating that thermal disorder might become important at larger temperatures, anticipating the melting process of the vortex glass phase.

DOI: 10.1103/PhysRevB.82.104506 PACS number(s): 74.25.Dw, 74.25.Ha, 74.25.Uv, 74.25.Wx

I. INTRODUCTION

Although a vortex state, in type-II superconductors, has been anticipated more than 50 years ago,[1] a great deal of theoretical and experimental efforts have been devoted to investigate the dynamics of those structures, its dependence on external excitations and on the inherent properties of the underlying superconducting material, such as inhomogeneities, commonly designated as static disorder.[2] As a matter of fact, the spacial distribution of vortex matter (VM) in superconductors is greatly influenced by the occurrence of inhomogeneities and/or imperfections.

It is well known that the presence of inhomogeneities in low-T_c and high-T_c superconductors turns out to be an important feature leading to a large current transport capability without dissipation. This is so because regions with less robust or even suppressed superconducting properties act as pinning centers, impeding the viscous motion of vortices in the presence of a transport current. However, such inhomogeneities not only affect the dynamic behavior of the magnetic flux lines; their presence has important consequences on the magnetic field versus temperature (H-T) phase diagram, since they suppress long-range translational order on the Abrikosov lattice.[2]

For imperfections whose size is on the order of the superconducting coherence length, the current theoretical perspective is that weak-disorder results on a vortex solid phase denominated Bragg Glass (BrG),[3,4] which retains the topological order of the flux line lattice but yields broadened diffraction peaks,[5] while uncorrelated strong disorder, like impurities and oxygen vacancies, results on a topologically disordered vortex glass (VG) phase.[6–15] This VG phase is expected to be truly superconducting: for low current densities, the pinning barriers become infinite, preventing any vortex motion, thus resulting in null resistivity.

II. PERCOLATIVE SUPERCONDUCTIVITY AND THE VG PHASE IN $Mg_{1-x}B_2$

Since the discovery of superconductivity in MgB_2 at 39 K,[16] a considerable progress in the understanding of the fundamental properties of this material has been accomplished. Regarding VM phases in single crystals, a quasiordered vortex structure has been observed at low dc fields,[17] i.e., the H-T diagram of such clean specimens has a region where the stable vortex phase is a BrG. Nonetheless, by tuning the amount of static disorder, the stabilization of a VG phase can be favored and, consequently, a BrG-VG transition, which is ordinarily associated with a peak in the critical current density (peak effect),[18] should become observable at fields smaller than the upper critical field, $H_{c2}(T)$. Besides, a vortex glass-vortex liquid (VL) VG-VL transition should also appear in the mixed phase of MgB_2 with random disorder.

Members of the $Mg_{1-x}B_2$ system with Mg deficiency in the range $0<x\leq 0.1$ exhibit percolative superconductivity; specimens with higher levels of Mg deficiency have an insulator like resistive response.[19] This behavior is a consequence of the tendency of Mg-deficient regions to form clusters, whose typical size grows with increasing x, so that percolative superconductivity is suppressed for larger amounts of deficiency. Since the typical cluster size falls within the 10 nm range for small values of x,[19] one would then expect to have the adequate environment—a superconductor with point defects—for probing the BrG-VG and/or VG-VL transitions of VM. In this work we study the magnetic phase diagram of three samples of the $Mg_{1-x}B_2$ system with static disorder, provided in practice by tuning the Mg content of the specimen. As discussed in the following sessions, we determined the melting line of the VG phase. The studied specimens do not present the so-called peak effect, from which we conclude that the BrG phase, although predictable, is not present.

III. SAMPLES AND EXPERIMENTAL METHOD

The polycrystalline samples of $Mg_{1-x}B_2$ with $0\leq x\leq 0.1$ employed in this study were prepared by solid-state reaction methods under high pressure, details of which were given in Ref. 19. Four samples with different deficiency content were studied, which were labeled with a roman numeral (I)–(IV), ordered according to increasing values of x: sample I—MgB_2, sample II—$Mg_{0.975}B_2$, sample III—$Mg_{0.925}B_2$, and

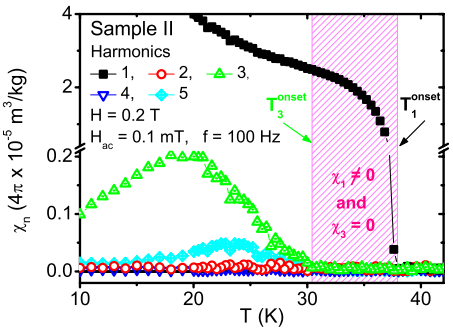

FIG. 1. (Color online) Temperature dependence of the harmonic susceptibilities, χ_n, for sample II, up to the fifth component, measured at $H=0.2$ T with $H_{ac}=0.1$ mT and $f=100$ Hz. The only relevant harmonics are odd, especially the first and the third. Data evidence the existence of a temperature window, $T_3^{onset} \leq T \leq T_1^{onset}$, within which the susceptibility is linear ($\chi_1 \neq 0$ and $\chi_3=0$).

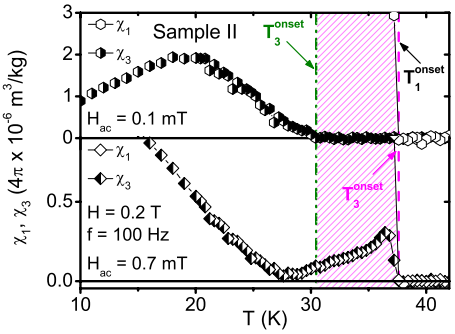

FIG. 2. (Color online) Curves of $\chi_1(T)$ and $\chi_3(T)$, for sample II, at different amplitudes of H_{ac} with $f=100$ Hz and $H=0.2$ T. Notice the difference in T_3^{onset} with the increase in H_{ac}.

sample IV—$Mg_{0.9}B_2$. Sample I, the pristine specimen, was included in the study as a reference.

To accomplish an accurate study of the influence of static disorder on the state of VM in $Mg_{1-x}B_2$ samples, we have employed harmonic analysis, determining the harmonic components of the ac magnetic susceptibility, χ_n. As the temperature decreases, χ_3 becomes nonzero below a field-dependent temperature $T_3^{onset}(H)$; warming up the sample, χ_3 vanishes reversibly at the same temperature, which we associate to the melting temperature of the VG phase. The association among any uneven behavior of the magnetic response—either the ac susceptibility or the magnetization—and a phase change in VM, has been exhaustively discussed in the literature.[20–24] A particularly instructive debate was maintained by Krusin-Elbaum *et al.*[22,24] and by Samoilov and Konczykowski,[23] regarding the melting of the Bose-glass phase in $YBa_2Cu_3O_{7-\delta}$ with columnar defects. It was argued that, at low amplitudes of the excitation field, the temperature at which the imaginary part of χ_1 peaks can be taken as the melting temperature. Although acceptable under certain circumstances, this holds only as an approximation, and the actual melting occurs at the onset of χ_3, which is also confirmed in the present work, as discussed below. As a matter of fact, vortex dynamics is generally influenced by frequency and amplitude of the excitation field, in such a way that whatever physical quantity is chosen to be monitored, it is mandatory to ensure that the response is not affected by the adjustable parameters of the probing field.

Measurements of χ_n were performed as a function of temperature, $\chi_n(T)$, up to the tenth order, for different values of the applied magnetic field, H. The amplitude, H_{ac}, and frequency, f, of the excitation field, where also taken as adjustable experimental parameters. Figure 1 exemplifies the magnitudes, $\chi_n=|\chi_n'+i\chi_n''|$ of the first five harmonics of the ac magnetic susceptibility for sample II. In this illustration one may notice that, apart from the fundamental, χ_1, the most relevant harmonic is the third, χ_3. It is worth mentioning that, in the absence of an applied magnetic field, the ac susceptibility should exhibit odd harmonics only.[25] Our experimental observation confirms this general result. As a matter of fact, even when large dc fields are present, the harmonic content is essentially odd. Thus, although we monitored all harmonics up to the tenth, only the first and third components are presented in the majority of the figures in this paper. The hatched region in Fig. 1 emphasizes the existence of a range of temperatures, $T_3^{onset} \leq T \leq T_1^{onset}$, at which the magnetic response of the system is linear. We identify T_1^{onset} with T_c, whose experimental values were determined to be (39.0 ± 0.5) K for sample I and (39.2 ± 0.2) K for the other three samples (II, III, and IV).

Next section presents our experimental results, starting from a detailed investigation on how the temperature interval of the linear magnetic response (i.e., $\chi_n=0$, $n \neq 1$) depends on H_{ac} and f. This study enabled us to establish the appropriate conditions for the employment of the third harmonic susceptibility technique to detect the VG-VL transition in the studied $Mg_{1-x}B_2$ samples. To conduct all magnetic measurements we employed two Quantum Design commercial magnetometers: Magnetic Property Measurement System (MPMS-5S) and the Physical Property Measurement System (PPMS-M6000). We have also used the ACMS module of the PPMS to measure transport properties, including curves of resistance as a function of the temperature, $R(T)$, for a fixed excitation current, I, and also current-voltage (I-V) curves, at several values of T and H.

IV. RESULTS AND DISCUSSION

A. Systematic study of χ_3—dependence of T_3^{onset} with H_{ac} and f

Figure 2 shows a comparison between curves of $\chi_1(T)$ and $\chi_3(T)$, obtained for sample II with two different amplitudes of the excitation field, both at $f=100$ Hz. This illustration reveals that T_3^{onset} tends to approach T_1^{onset} with the increment of H_{ac}.

A thorough study about the behavior of T_3^{onset} with H_{ac} was conducted by means of a large number of measurements of $\chi_3(T)$ subject to a variety of combinations of the excitation parameters. Selected parts of this study are shown in Fig. 3 with data taken at different values of the excitation amplitude for fixed values of f (100 Hz) and H (0.2 T). Notice that while T_1^{onset} remains approximately constant at (37.7 ± 0.4) K, T_3^{onset} decreases sharply to (30.6 ± 0.4) K for values of H_{ac} around 0.1 mT and below. Thus, in the limit of

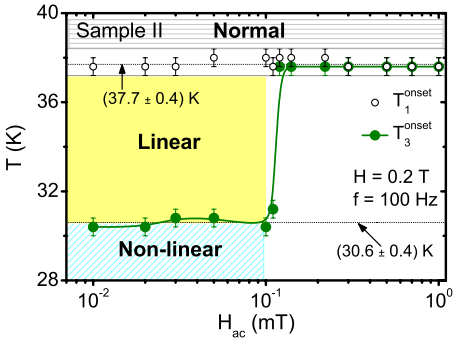

FIG. 3. (Color online) Dependence of T_1^{onset} and T_3^{onset} with H_{ac} for sample II. The arrows indicate the approximately constant values of T_1^{onset} and T_3^{onset}.

low excitation, one can easily identify, in the TH_{ac} plane, two different regimes of the ac magnetic response, one of which is characterized by $\chi_3=0$ and $\chi_1\neq 0$ (linear) and the other (nonlinear) having nonzero χ_3 and χ_1. The normal state, where $\chi_1=\chi_3=0$, is also indicated. For $H_{ac}>0.1$ mT, a field-induced nonlinear response is obtained, as a consequence of the excessive amplitude of the excitation field. The steplike form of $T_3^{onset}(H_{ac})$—possibly associated to the fact that too many vortices are forced in and out while the sample is about to reach its normal state—further emphasizes that an excessive amplitude of the probing field influences vortex dynamics and should not be used in a study like this.

The frequency dependence of T_3^{onset} was also investigated for all studied samples. This part of the study is illustrated here with data taken with sample II: the amplitude H_{ac} was maintained constant at 0.02 mT—deep into the region where, at 100 Hz, the excitation field did not induce spurious nonlinearities (Fig. 3)—and $\chi_3(T)$ measured at various frequencies. In Fig. 4, curves of χ_3, obtained at two different frequencies, are confronted. Equivalently to the result suggested in Fig. 2, we observe that increasing the excitation frequency causes T_3^{onset} to approach T_1^{onset}. The frequency dependence of T_3^{onset} is shown in Fig. 5. Such panel reveals that for $f\leq 100$ Hz, T_3^{onset} stabilizes in a value compatible with the one obtained through the study of the amplitude dependence. Therefore, below this threshold frequency, one can surely distinguish, in the Tf plane, a genuine threshold between the linear and nonlinear regimes of VM.

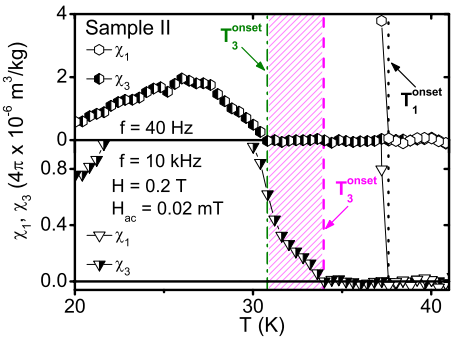

FIG. 4. (Color online) Comparison between curves of $\chi_1(T)$ and $\chi_3(T)$ obtained at different frequencies of the ac field. Although measurements have been accomplished in the limit of low H_{ac}, notice the variation in T_3^{onset} with f.

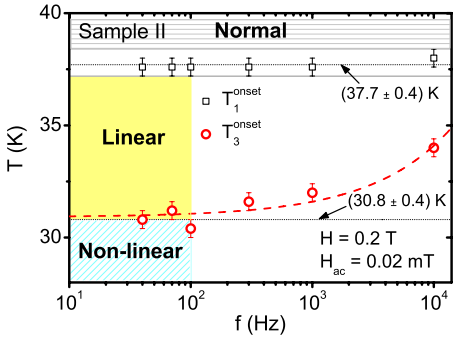

FIG. 5. (Color online) Dependence of T_1^{onset} and T_3^{onset} with f. The dashed line is an adjustment of Eq. (1) to the experimental data with $T_3^{onset}(f\to 0)=(30.9\pm 0.2)$ K and $\delta=(0.67\pm 0.03)$. The approximately constant value of T_1^{onset} and the asymptotic value of T_3^{onset} are arithmetic averages. Notice the similarity between the value of T_3^{onset} and the adjusted parameter $T_3^{onset}(f\to 0)$.

Moreover, data in Fig. 5 emphasizes that $T_3^{onset}(f)$ can be described by Eq. (1)

$$T_3^{onset}(f)=T_3^{onset}(0)+Af^{\delta}, \tag{1}$$

where A, $T_3^{onset}(0)$, and δ are fitting parameters. This expression has the exact format of that derived by Fisher and collaborators (VG model)[6,7] for the frequency dependence of the irreversibility temperature, T_{ir}, in the limit of $f\to 0$. The correspondence is straight: $T_3^{onset}(0)$ is the glass temperature and $\delta=1/[(z-1)\nu]$, being z the dynamical and ν the correlation-length critical exponents, respectively, associated with the VG-VL transition. Equation (1) was adjusted to the experimental data (dashed line in Fig. 5), leading to $T_3^{onset}(0)=(30.9\pm 0.2)$ K and $\delta=(0.67\pm 0.03)$. The obtained value for the exponent is in excellent agreement with the value ($\delta=2/3$) derived through a mean-field approximation for the VG model.[2] We take this result as an important evidence that Mg deficiency actually stabilizes the VG phase for low-x samples of the studied system.

The systematic investigation of the χ_3 dependence on frequency and amplitude of the excitation field indicates the proper conditions for employment of the third harmonic susceptibility in the study of vortex dynamics in type-II superconductors. As experimentally demonstrated, its applicability is restricted to the limit of low-amplitude/low-frequency excitation. The threshold values H_{ac}^{th}, and f_{th}, below which T_3^{onset} is independent of such parameters, were determined for each of the samples studied in this work and are listed in Table I.

Figure 6 shows a comparison between curves of $\chi_1''(T)$ and $\chi_3(T)$ for sample II. There one can see that the onset temperature of χ_1'', indicated by the dashed line, is higher than T_3^{onset}. This means that between those temperatures, there is dissipation ($\chi_1''>0$) which, however, is linear with the excitation amplitude (see region labeled "Linear" in Figs. 3 and 5), since $\chi_3=0$. Such behavior is typical of the vortex liquid phase. For $T<T_3^{onset}$, where $\chi_3>0$, VM is in the glass phase. On the other hand, below the glass temperature, $T_g(H)$, it is well known that the electric field at low current densities ($j\to 0$) is nonlinear, $E\propto\exp[-(J_0/j)^{\mu}]$.[6,7] Exactly at

TABLE I. Threshold values of H_{ac} and f, below which one can assure that the excitation field has no influence on the experimental results.

Sample	H_{ac}^{th} (mT)	f_{th} (Hz)
II	0.1	100
III	0.008	100
IV	0.01	100

T_g, the current-voltage (I-V) characteristic curve is given by a power law and, for temperatures above T_g, a linear (Ohmic) behavior is expected, $E \propto j$. In terms of magnetic measurements, we equally identified, within the limits of low excitation, two different regimes of VM, whose response is nonlinear below T_3^{onset} and linear above it. In the latter regime, the energy dissipation, coming from the viscous motion of vortices, is linear (Fig. 6), as predicted by the VG model. We take this as a second sound evidence that, at lower temperatures, VM is at the vortex glass phase.

Experimentally, the melting line of the vortex glass, i.e., the VG-VL boundary in the H-T phase diagram, $H_m(T)$, was determined by measuring—in the low excitation limit—$\chi_3(T)$ for several values of the dc magnetic field. As a matter of fact, a linear response is expected at very low excitations, even in the vortex glass phase. Our data show that, below the melting frontier, the ac susceptibility has a linear appearance up to $H_{ac} \sim 0.05$ mT. This linearity could be expressed in terms of the quality of a linear fitting, but the harmonic analysis is a much more sensitive approach, and shows that a small nonlinear contribution develops ($\chi_3 \neq 0$) below the melting line. One could possibly ascribe this behavior to the fact that the clusters promoting stabilization of the vortex glass phase are not really point defects, but somewhat larger than the size of individual vortices. Besides, traces of some weak ordering of the clusters were described by Sharma and co-workers,[19] what could conceivably be considered as the reason for the observed nonlinear behavior.

B. H-T phase diagram

As discussed above, the frequency and the amplitude of the excitation field can both affect the temperature below which χ_3 emerges from zero. In order to assure the best possible signal-to-noise ratio without compromising the actual significance of the experiment, one has to maximize H_{ac} without exceeding the characteristic threshold of each sample (Table I). Having this in mind, we have chosen H_{ac} =0.02 mT, 0.008 mT, and 0.007 mT, for samples II, III, and IV, respectively. The frequency was set to f=100 Hz for all melting lines determined in this work.

Figure 7 depicts the H-T phase diagram obtained for the $Mg_{1-x}B_2$ samples. For the pristine (i.e., without Mg-deficiency) specimen, sample I, χ_3 has nonzero values at all temperatures in the superconducting phase, i.e., the melting line of VM, $H_m(T)$, coincides with $H_{c2}(T)$. When defects are present, however, a randomly distributed static disorder scenario is set and, as discussed earlier in this paper, a VG phase

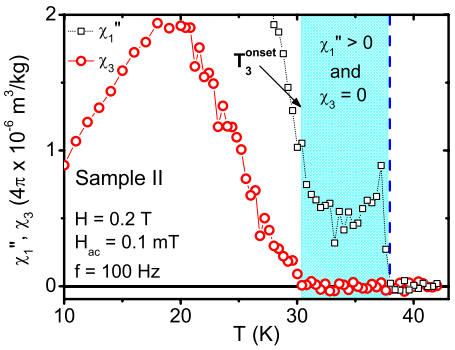

FIG. 6. (Color online) Curves of $\chi_1''(T)$ and $\chi_3(T)$ for sample II. The measurement parameters were: H_{ac}=0.1 mT, f=100 Hz, and H=0.2 T. A range of temperatures where the dissipation is linear, i.e., $\chi_1'' > 0$ and $\chi_3 = 0$, is emphasized by the vertical rectangle.

is stabilized. Solid and dashes lines are fittings whose origin and meaning we discuss later in the text. As seen in Fig. 7, the relative area of the liquid phase decreases for increasing x, what we interpret as a consequence of an increase on the pinning potential for larger amounts of Mg deficiency. In fact, this reasonable assumption is consistent with our experimental determination of the pinning potential, U_p, for the studied samples, as presented and discussed in the following paragraphs.

An estimate of U_p was accomplished examining how the peak temperature of $\chi_1''(T)$, T_p, corresponding to the situation of maximum dissipation of energy, resulting from the viscous motion of the magnetic flux lines, evolves for different values of f. For the thermally activated vortex motion (flux creep), T_p is shifted to a higher value with the increase in f. This shift can be described by an Arrhenius law[26,27]

$$f = f_0 \exp[-U_p/k_B T_p], \tag{2}$$

where f_0 is a characteristic frequency, k_B is the Boltzmann constant, and $U_p = U_p(T,H,J)$ is the activation energy for depinning, which is the height of the potential barrier that vortices must overcome when hopping from one pinning site to another.

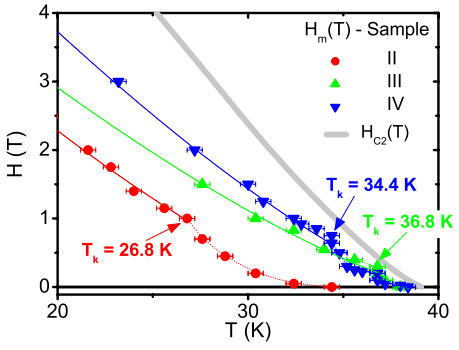

FIG. 7. (Color online) VG-VL threshold for the studied samples of $Mg_{1-x}B_2$. $H_{c2}(T)$ is an average line that represents the experimental data obtained for all samples. Experimental points were adjusted by a power law (solid lines), Eq. (3) with γ=4/3 (vortex-glass model). The dashed line is an adjustment of Eq. (4) to the high-temperature data (see text).

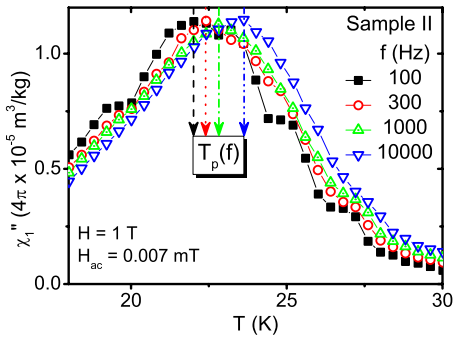

FIG. 8. (Color online) Curves of $\chi_1''(T)$, for sample II, measured at a dc field of 1 T, H_{ac}=0.007 mT and frequencies of 100, 300, 1000, and 10 000 Hz.

Experimentally, measurements of $\chi_1''(T)$, for samples I, II, III, and IV, were performed with H_{ac}=0.007 mT at different values of H. As an example, we illustrate, in Fig. 8, $\chi_1''(T)$ curves measured at different frequencies for sample II. Notice that T_p is shifted to higher temperatures as f is increased. Figure 9 presents the dependence of $\ln(f)$ with $1/T_p$ for the studied Mg-deficient samples. The solid lines are linear fittings from which we determine the activation energy, U_p, according to Eq. (2). The obtained values of U_p are plotted against x in the inset of Fig. 9. It is worth mentioning that T_p for sample I does not change with f, as expected for a specimen that does not exhibit the VG phase which, for the other samples, is stabilized by the presence of point defects. This assures that the activation energy determined for the two-level systems described by the Arrhenius behavior, is actually related to potential barriers created by Mg deficiency, inexistent in the pristine sample.

We now focus on the format of the $H_m(T)$ contour. In general,[7,28–30] critical borders like the irreversibility, melting and glass lines, can be empirically described by a simple power law

$$H_{cr}(T) = H_0[1 - T/T_{cr}(0)]^{\gamma}, \tag{3}$$

where $T_{cr}(0)$ is the temperature of irreversibility, melting or glass, respectively, at H=0, H_0 is the value of $H_{cr}(T)$ extrapolated to T=0 and γ is a fitting parameter. In the present case, γ was kept fixed at 4/3, which is the value predicted for the VG-VL line.

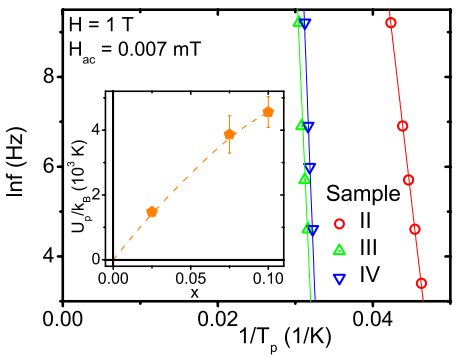

FIG. 9. (Color online) Arrhenius diagram, $\ln(f)$ versus $1/T_p$, obtained for samples II, III, and IV. The solid lines (main panel) are linear fittings. Dependence of U_p with x is shown in the inset. The dashed line is just a guide to the eyes and extrapolates to zero as an indication that the pristine sample has a frequency-independent T_p (see text).

TABLE II. Parameters obtained from fittings using Eqs. (3) and (4).

Sample	H_0 (T)	$T_3^{onset}(0)$ (K)	B (T/K^2)	T_0 (K)
II	(7.3 ± 0.2)	(34.4 ± 0.3)	$(1.37 \pm 0.03)10^3$	(1.94 ± 0.09)
III	(7.4 ± 0.4)	(39.5 ± 0.3)	$(1.7 \pm 0.2)10^{36}$	(0.4 ± 0.1)
IV	(9.5 ± 0.2)	(39.5 ± 0.5)		

The experimental points of $H_m(T)$ were modeled by Eq. (3) with $T_3^{onset}(H=0)$ in place of $T_{cr}(0)$. As shown in Fig. 7, this power law (solid lines) provides a good fitting to the low-temperature/high-field data. However, it overestimates the $H_m(T)$ borders in the high-temperature/low-field regime. At high temperatures, the format of $H_m(T)$, simulated by the dashed lines in Fig. 7, obeys an expression of the type

$$H(T) = BT^2 \exp(-T/T_0), \tag{4}$$

where B and T_0 are fitting parameters. This equation is based on the theoretical model developed by Lopatin and Vinokur,[31] which predicts the anticipation of the melting transition of VM—which, for the present case, is the VG-VL threshold, $H_m(T)$—as a consequence of temperature-induced depinning of vortices. The parameters that optimize these fittings for each sample are listed in Table II. As a matter of fact, the high-temperature portion of the melting line for sample IV is not as smooth as for the other two Mg-deficient samples, what is conceivably due to an excessive degree of disorder; although a kink temperature is recognizable from the data, Eq. (4) would not provide a good quality fitting to the experimental points.

This type of thermally assisted depinning, observed previously by Banerjee and collaborators[32] in the VM phase diagram of BSCCO-2212 with columnar defects, is present in our experimental data, suggesting that the influence of defects on the vortex dynamics becomes secondary in the high-temperature/low-field region, where the $H_m(T)$ frontier is shifted toward lower temperatures. We identified such regime of the melting line, which is adequately adjusted by Eq. (4), as a thermally induced melting of the VG phase in $Mg_{1-x}B_2$. It is important to emphasize, however, that the thermally assisted depinning of Eq. (4) was predicted by Lopatin and Vinokur for a three-dimensional vortex system in a superconducting material with columnar defects, exactly as in the case verified by Banerjee *et al.* In our samples, the corresponding defects are not columns but tiny clusters, randomly distributed throughout the volume. It is conceivable though that the pinning efficiency of such clusters is also diminished by increasing temperatures, so that an anticipated melting is likely to occur.[33]

The two-regime melting line represented by the $H_m(T)$ curves shown in Fig. 7, indicate that, at low temperatures, the VG state has properties dependent on the type and efficiency of the static disorder in the system. Figure 10(a)

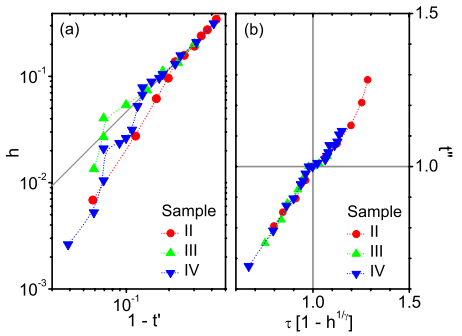

FIG. 10. (Color online) (a) Scaling of the $H_m(T)$ curves, privileging the low-temperature data. Here, $t'=T/T_3^{onset}(0)$ and $h=H/H_0$. (b) In this panel, the variables are different from those in (a): $t''=T/T_k$ and $\tau=T_3^{onset}(0)/T_k$.

shows a scaling of the $H_m(T)$ curves, with the low-temperature/high-field data collapsed. In such panel it becomes unambiguous that for all Mg-deficient samples studied, the experimental points at low temperatures obey a power law, while those at higher temperatures deviate from this behavior at the point where a thermally assisted depinning crossover sets in. The reduced variables were defined as $t'=T/T_3^{onset}(0)$ and $h=H/H_0$. Figure 10(b) is an alternative way of scaling the $H_m(T)$ curves with a different combination of the variables. A new parameter is introduced, the kink temperature T_k, above which thermal depinning occurs (values of T_k for each of the studied samples are also indicated in Fig. 7). For this scaling, we define the variable $t''=T/T_k$ and the dimensionless parameter $\tau=T_3^{onset}(0)/T_k$. As a result, one can notice in panel (b) of Fig. 10 that the $H_m(T)$ contours collapse throughout the entire temperature range. The existence of two distinct behaviors for $H_m(T)$—below and above $t''=1$—is also evidenced. The thermally induced depinning regime occurs for $t''\geq 1$ while the $t''\leq 1$ region corresponds to the power-law domain discussed above.

Another important issue is to identify possible connections among the VG-VL lines determined in this work and the irreversibility line (IL), $H_{ir}(T)$. Figure 11 displays $H_m(T)$ and $H_{ir}(T)$ for samples (a) II and (b) IV. These specimens represent extreme situations in our study: in (a), $H_{ir}(T)$ and $H_m(T)$ are significantly different whereas in (b) they represent basically the same contour. To better understand this difference for sample II, we performed transport measurements. As an example of the results of the transport study, Fig. 12 shows the temperature dependence of the resistance, $R(T)$, for sample II, obtained in the limit of low excitation, i.e., low transport current ($i_t\rightarrow 0$), and in the presence of a dc field of 1 T. For $T\leq 26.3$ K, $R(i_t\rightarrow 0)\approx 0$, which means that, up to 26.3 K, the material is in a truly superconducting state, allowing transport of electric current without dissipation. We include the point corresponding to this state $[(26.3\pm 0.4)\ \mathrm{K};1\ \mathrm{T}]$ in the H-T phase diagram of Fig. 11(a), which should be compared with the experimental data $[(26.8\pm 0.4)\ \mathrm{K};1\ \mathrm{T}]$ corresponding to $H_m(T)$. This indicates that VM experiences dissipative dynamics, just above the melting line, in the liquid state.

In addition, we have also conducted experiments to measure I-V curves, as those shown in Fig. 13(a) for sample II,

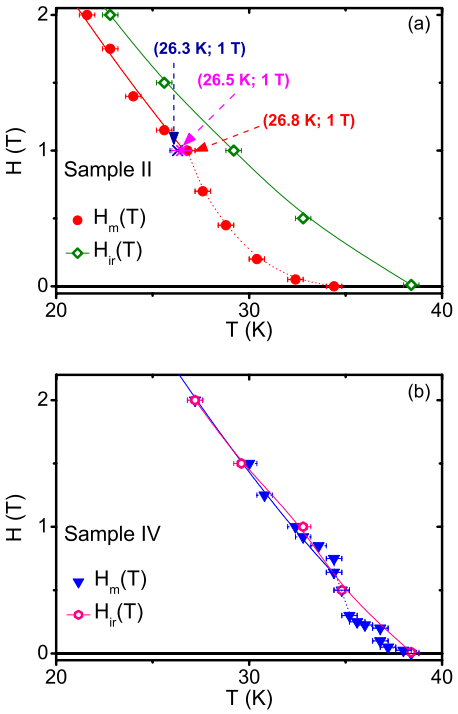

FIG. 11. (Color online) Comparison between the $H_m(T)$ and $H_{ir}(T)$ thresholds obtained for samples (a) II and (b) IV. We used the $M(T)$ technique to determine the $H_{ir}(T)$ lines.

obtained for several values of the temperature in a dc field of 1T. It is relatively simple to verify that, for $T\geq 26$ K, these curves exhibit a linear behavior. To determine this threshold temperature, we adjusted the experimental data with an expression of the type $V=dI$, where d is a constant. We then monitored the quality of the fittings for each temperature, $Q(T)$, as illustrated in Fig. 13(b). Using the criterion of 0.1%, i.e., assuming that good linear fittings are those with $Q\geq 0.999$, we determined 26 K as the threshold value of T below which the I-V response is no longer linear. The hatched region in Fig. 13(b) represents the tolerance of 0.1%.

This linear characteristic, exhibited by the I-V curves of sample II for $T\geq 26$ K, reveals that even in the limit of low excitation ($i_t\rightarrow 0$), pinning centers present in the material are no longer effective in preventing the viscous motion of vortices, and $R(i_t\rightarrow 0)\neq 0$. The threshold for this linear response, represented by the coordinates

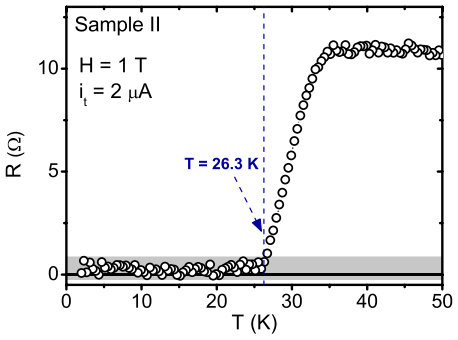

FIG. 12. (Color online) $R(T)$ measured at $H=1$ T for sample II.

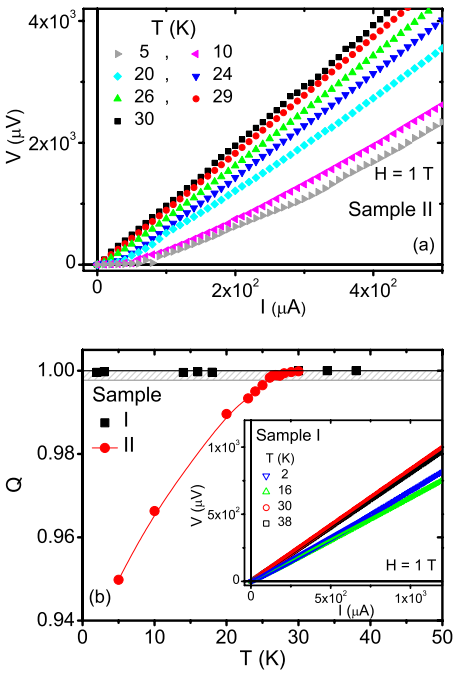

FIG. 13. (Color online) (a) *I-V* diagram, obtained at $H=1$ T for sample II. (b) Dependence of Q with T for samples I and II. In the inset, the linear behavior of all of the *I-V* curves obtained for sample I is illustrated.

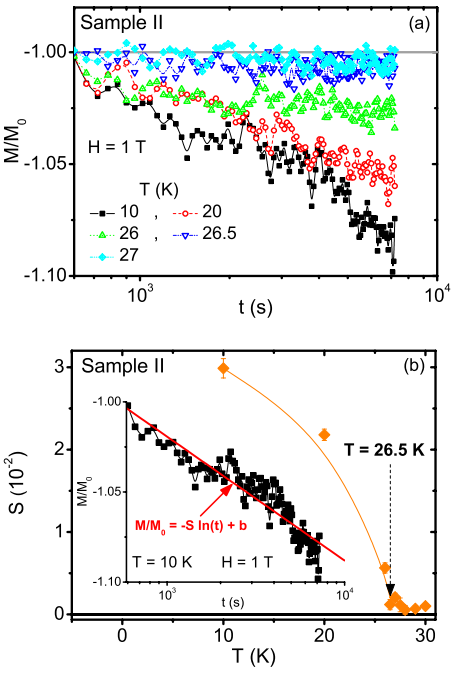

FIG. 14. (Color online) (a) $M(t)$ curves for sample II. Such curves were normalized to the remanent magnetization M_0 measured 10 min after changing the field. (b) Decay rate as a function of the temperature. In the inset, we show how S was determined for $M(t)$ measured at $H=1$ T and $T=10$ K.

$[(26.0\pm0.4)\ \mathrm{K};1\ \mathrm{T}]$, although not inserted in the already crowded Fig. 11(a), should also be compared with the special points represented there, like the inception of the linear magnetic response determined by means of measurements of the third harmonic $[(26.8\pm0.4)\ \mathrm{K};1\ \mathrm{T}]$. In view of this result, it becomes evident that the IL for sample II is not the boundary below which VM is in a state characterized by essentially pinned vortices, for which $R(i_t\rightarrow0)\approx0$. As a matter of fact, this feature applies to the vortex glass phase, upperbounded by $H_m(T)$, which is, therefore, the true melting frontier.

In contrast to the *I-V* curves measured for sample II, the pristine specimen (sample I) exhibits a linear behavior measured at all temperatures, as shown in the inset of Fig. 13(b) with curves taken in a dc field of 1T. Linear *I-V* characteristics, i.e., $I\propto V$, are typical of an ideal (without defects) superconducting material. The solid lines are fittings of the expression $V=dI$ to the experimental points. The nearly constant value of $Q(T)$ for sample I, also shown in Fig. 13(b), means that the quality of the fittings remains close to ideal in the whole range of temperatures, i.e., the experimental points for sample I form a straight line going through zero.

Vortex trapping allows the stabilization, at least temporarily, of a nonuniform distribution of magnetic flux in the whole volume of the superconducting material. Experimentally, the evolution of this metastable state toward thermodynamic equilibrium is evidenced by magnetic relaxation.[34] We have used relaxation measurements, $M(t)$, as an additional tool to study the dynamic behavior of VM in samples II, III, and IV. Isothermal $M(t)$ measurements[35] were conducted after a field-cooled process followed by a decrease on the applied field of $\Delta H=1$ T. Figure 14(a) illustrates $M(t)$ for sample II, revealing that the normalized logarithmic decay rate $S=-(1/M_0)dM/d\ln(t)$ diminishes when the temperature is increased. In Fig. 14(b), $S(T)$ is presented; the temperature below which the magnetization decays logarithmically in time is $T=26.5$ K. A point with coordinates $[(26.5\pm0.5)\ \mathrm{K};1\ \mathrm{T}]$ was included in the *H-T* diagram of Fig. 11(a). One can see that, within experimental accuracy, it belongs to the $H_m(T)$ frontier. This is not surprising: below the VG-VL boundary, vortex motion is limited by pinning wells and the glassy phase is a consequence of the random distribution of the pinning centers. Upon reduction in the applied field, relaxation derives from vortex rearrangements resulting from a competition between pinning and thermal energies, as the system evolves to a metastable equilibrium. Above that frontier, however, vortices are freed from the attractive wells and competition ceases so that the system achieves its most favorable configuration at once and no sizeable relaxation is expected to occur.

V. FINAL REMARKS

The results obtained from the systematic analysis of the third harmonic allowed us to verify that the appropriate choice of the experimental parameters—amplitude and frequency of the excitation field—is extremely important when one wants to study the dynamic behavior of vortex matter by means of measurements of higher-harmonic susceptibilities. We have distinguished, in the limit of low excitation, the genuine transition between the vortex glass and the vortex liquid phases. The upper limit to the vortex glass state is strongly influenced by the type and density of static disorder

existent in the superconducting material and is shifted to higher values of fields and temperatures with the increase in disorder. Furthermore, we have verified, for a pristine sample, the coincidence between the VG-VL contour and $H_{c2}(T)$, meaning that in the absence of inhomogeneities, the stabilization of the vortex glass phase of vortex matter is unfavored.

The irreversibility line, frequently identified in the literature as the melting line of vortex matter, has been compared to the VG-VL threshold. Although both lines may constitute the same contour for the sample with higher Mg deficiency (sample IV), it is not the case for the other nonpristine specimens (samples II and III). In addition, magnetic relaxation studies and measurements of electrical transport evidenced that, in the neighborhood of the VG-VL line and above, vortices are in an equilibrium configuration—i.e., its dynamics is not affected by the static disorder present in the material. Also, we were able to verify the existence of a correlation between a linear *I-V* behavior, $I \propto V$, and the regime of linear magnetic response, $\chi_3=0$ and $\chi_1 \neq 0$, determined by means of third harmonic measurements. This result confirms that, indeed, vortex matter is in the vortex glass phase below $H_m(T)$, since in the low-excitation limit—low transport current or low ac magnetic field—the electrical and magnetic responses are nonlinear below T_3^{onset} and linear above that threshold. It should be also mentioned here that the apparent contradiction of a nonrelaxing magnetization below the irreversible line, $H_m(T)<H<H_{ir}(T)$, was already discussed in an earlier paper[36] with data on samples similar to the ones employed here. That previous work has shown that $M(t)$ relaxation is different for vortices entering and leaving the sample, although both processes can be suitably fitted assuming a Bean-Livingston surface barrier mechanism.

We have also found that, in the high-temperature/low-field region of the *H-T* phase diagram, the studied border has two different regimes, and the VG-VL limit is anticipated for $T>T_k$. We have interpreted the occurrence of this anticipation as a result of the competition between two different types of disorder—static and thermal—in the material. Hence, the *H-T* phase diagram of Mg-deficient samples, as the ones studied here, is such that at different regions one type of disorder is more important than the other, what is manifested by the existence of a kink temperature separating the two regimes of the VG-VL contour.

As a last remark, we would also like to emphasize that all evidences collected in this work confirm that the Mg-deficient clusters of samples II, III, and IV are responsible for the stabilization of the vortex glass phase in those specimens. The portion occupied by the vortex glass state in the phase diagram is expanded as x increases and, equally important, it is absent for the pristine MgB_2 sample.

ACKNOWLEDGMENTS

The authors wish to acknowledge Peter Sharma for fruitful discussions on the percolative nature of superconductivity in the $Mg_{1-x}B_2$ system. Financial support from Brazilian agencies FAPESP and CNPq is also acknowledged. Work at Rutgers was supported by the National Science Foundation Grant No. NSF-DMR-0804109.

*Present address: Departamento de Física, Universidade Federal de Santa Maria, 97105-900 Santa Maria, RS, Brazil.

[1] A. A. Abrikosov, Sov. Phys. JETP **5**, 1174 (1957).
[2] G. Blatter, M. V. Feigel'man, V. B. Geshkenbein, A. I. Larkin, and V. M. Vinokur, Rev. Mod. Phys. **66**, 1125 (1994).
[3] T. Giamarchi and P. Le Doussal, Phys. Rev. B **52**, 1242 (1995).
[4] T. Giamarchi and P. Le Doussal, Phys. Rev. B **55**, 6577 (1997).
[5] T. Klein, I. Joumard, S. Blanchard, J. Marcus, R. Cubitt, T. Giamarchi, and P. Le Doussal, Nature (London) **413**, 404 (2001).
[6] M. P. A. Fisher, Phys. Rev. Lett. **62**, 1415 (1989).
[7] D. S. Fisher, M. P. A. Fisher, and D. A. Huse, Phys. Rev. B **43**, 130 (1991).
[8] R. H. Koch, V. Foglietti, W. J. Gallagher, G. Koren, A. Gupta, and M. P. A. Fisher, Phys. Rev. Lett. **63**, 1511 (1989).
[9] R. H. Koch, V. Foglietti, and M. P. A. Fisher, Phys. Rev. Lett. **64**, 2586 (1990).
[10] P. L. Gammel, L. F. Schneemeyer, and D. J. Bishop, Phys. Rev. Lett. **66**, 953 (1991).
[11] H. Safar, P. L. Gammel, D. J. Bishop, D. B. Mitzi, and A. Kapitulnik, Phys. Rev. Lett. **68**, 2672 (1992).
[12] C. Dekker, W. Eidelloth, and R. H. Koch, Phys. Rev. Lett. **68**, 3347 (1992).
[13] J. M. Roberts, B. Brown, B. A. Hermann, and J. Tate, Phys. Rev. B **49**, 6890 (1994).
[14] L. Hou, J. Deak, P. Metcalf, and M. McElfresh, Phys. Rev. B **50**, 7226 (1994).
[15] L. Hou, J. Deak, P. Metcalf, M. McElfresh, and G. Preosti, Phys. Rev. B **55**, 11806 (1997).
[16] J. Nagamatsu, N. Nakagawa, T. Muranaka, Y. Zenitani, and J. Akimitsu, Nature (London) **410**, 63 (2001).
[17] M. R. Eskildsen, M. Kugler, G. Levy, S. Tanaka, J. Jun, S. M. Kazakov, J. Karpinski, and Ø. Fischer, Physica C **385**, 169 (2003).
[18] M. Angst, R. Puzniak, A. Wisniewski, J. Jun, S. M. Kazakov, and J. Karpinski, Phys. Rev. B **67**, 012502 (2003).
[19] P. A. Sharma, N. Hur, Y. Horibe, C. H. Chen, B. G. Kim, S. Guha, M. Z. Cieplak, and S-W. Cheong, Phys. Rev. Lett. **89**, 167003 (2002).
[20] L. Krusin-Elbaum, L. Civale, F. Holtzberg, A. P. Malozemoff, and C. Feild, Phys. Rev. Lett. **67**, 3156 (1991).
[21] R. A. Hein, T. L. Francavilla, and D. H. Liebenberg, *Magnetic Susceptibility of Superconductors and Other Spin Systems* (Plenum, New York, 1991).
[22] L. Krusin-Elbaum, L. Civale, G. Blatter, A. D. Marwick, F. Holtzberg, and C. Feild, Phys. Rev. Lett. **72**, 1914 (1994).
[23] A. V. Samoilov and M. Konczykowski, Phys. Rev. Lett. **75**, 186 (1995).
[24] L. Krusin-Elbaum, G. Blatter, and L. Civale, Phys. Rev. Lett. **75**, 187 (1995).
[25] L. Ji, R. H. Sohn, G. C. Spalding, C. J. Lobb, and M. Tinkham,

Phys. Rev. B **40**, 10936 (1989).
[26] L. Fàbrega, J. Fontcuberta, L. Civale, and S. Piñol, Phys. Rev. B **50**, 1199 (1994).
[27] G. Pasquini, L. Civale, H. Lanza, and G. Nieva, Phys. Rev. B **59**, 9627 (1999).
[28] Y. Yeshurun and A. P. Malozemoff, Phys. Rev. Lett. **60**, 2202 (1988).
[29] M. Tinkham, Phys. Rev. Lett. **61**, 1658 (1988).
[30] Y. Xu and M. Suenaga, Phys. Rev. B **43**, 5516 (1991).
[31] A. V. Lopatin and V. M. Vinokur, Phys. Rev. Lett. **92**, 067008 (2004).
[32] S. S. Banerjee, A. Soibel, Y. Myasoedov, M. Rappaport, E. Zeldov, M. Menghini, Y. Fasano, F. de la Cruz, C. J. van der Beek, M. Konczykowski, and T. Tamegai, Phys. Rev. Lett. **90**, 087004 (2003).
[33] V. M. Vinokur (private communication).
[34] Y. Yeshurun, A. P. Malozemoff, and A. Shaulov, Rev. Mod. Phys. **68**, 911 (1996).
[35] $M(t)$ is the *as-measured* total magnetization.
[36] W. A. C. Passos, P. A. Sharma, N. Hur, S. Guha, S.-W. Cheong, and W. A. Ortiz, Physica C **408-410**, 853 (2004).